The 2025 World Congress on
Advances in Structural Engineering and Mechanics (ASEM25)
BEXCO, Busan, Korea, August 11-14, 2025

Analytical study on the causes of cracks found at the end of hangers in a through type steel arch bridge

*Yuma Nagata[1)] and Takeshi Saigyo[2)], Shozo Nakamura[3)], Toshihiro Okumatsu[3)], Takafumi Nishikawa[4)]

[1) 3) 4)] Nagasaki University, Nagasaki, Japan
[2)]PAL Consulting Structural Engineers, Nagasaki, Japan
[1)] bb54125209@ms.nagasaki-u.ac.jp

ABSTRACT

Cracks were observed at the ends of hangers of a steel arch bridge in Nagasaki Prefecture. In this study, eigenvalue analysis was conducted to investigate the cause of the cracks, and the vibration modes were identified. Forced displacement analyses were performed by applying a displacement of 20 mm to the node with the maximum displacement in each vibration mode and similar displacements to the vibration mode to all other nodes. The bending and axial stresses at the hanger ends, where the cracks were found, were examined before and after the thickness loss due to corrosion. Additionally, the natural frequency of the hanger was determined and compared with that of the entire bridge vibration mode. This result suggests that the two were not resonant.

1. INTRUDUCTION

In recent years, the number of reported damage cases in bridges that are currently in service has steadily increased. Many of these bridges approach the time of replacement or major repair. Among the priority-managed bridges in Nagasaki Prefecture, Japan, cracks have been identified in the hangers of through-type steel arch bridges. Considering the structural characteristics of these bridges, such damage cannot be overlooked, as it could potentially lead to serious failures, such as bridge collapse.

The subject of this study is a through-type steel Langer arch bridge with a span length of 150 m and a width of 8.7 m. Cracks were detected at the ends of the fourth hanger from the bearing, and all occurred near the gusset plates. In addition, section loss due to corrosion was observed. Based on these observations, it was inferred that the

---

[1)] Graduate Student
[2)] Deputy Director, First Structural Design Department
[3)] Professor
[4)] Associate Professor

cracks were caused by a combination of bending and axial stresses induced by wind-induced vibrations, along with stress concentration due to corrosion.

According to Miki et al. (1988), in through-type arch bridges, excluding the wind-induced vibrations of hangers, structural damage is frequently observed around the connections between the arch or vertical members and transverse floor beams. Fatigue cracks were observed at the weld terminations on the web side of the girders or arch ribs, ends of the floor beams, and connection plates. Furthermore, it was found that deformations tend to concentrate at the joints between the arch rib and end floor beam due to the longitudinal movement of the deck system. Differential displacements between girders on either side also generate secondary stresses at the connections between the floor beams and girders.

In this study, a global finite element model of the target bridge was developed to investigate the cause of crack initiation. Subsequently, eigenvalue analyses were performed to identify the natural frequencies and displacement modes of the entire bridge, including those corresponding to the hanger where the cracks occurred. Forced displacement analyses were then conducted using the maximum vertical displacement observed during a typhoon. Finally, the normal stresses before and after corrosion were calculated using the bending moment and axial force for both the corroded and uncorroded cross sections.

2. CRACK DETAILS

The target bridge is a through-type steel Langer arch road bridge with a span length of 150 m and a width of 8.7 m. It was completed in 1986, and 44 years have passed since it started its service. Fig.1 presents a photograph of the target bridge, and Fig.2 shows its general arrangement drawing.

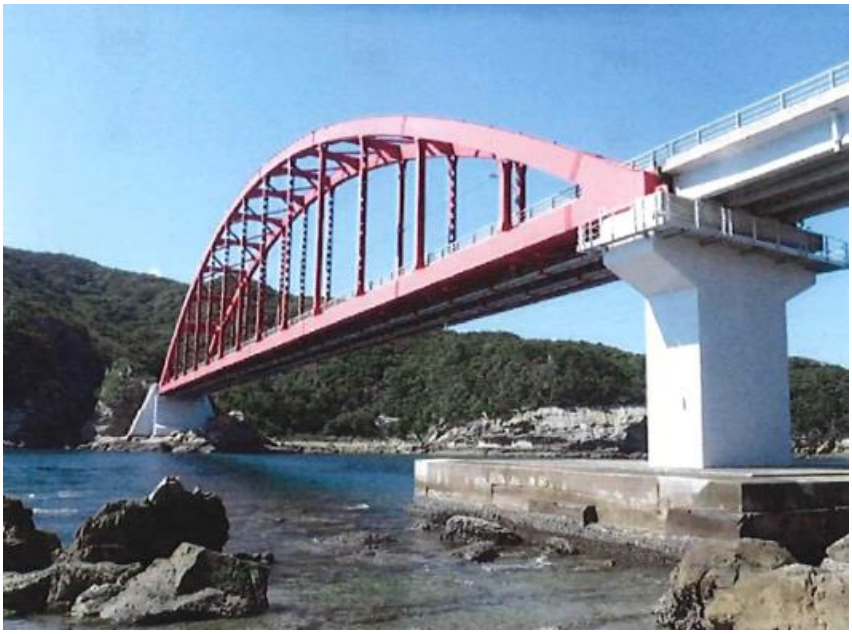

Fig.1 Photograph of the target bridge

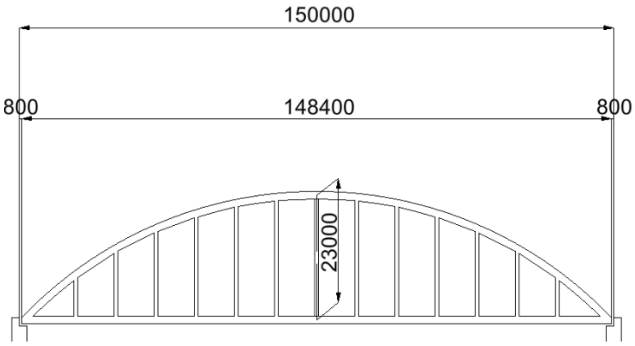

a) Side view

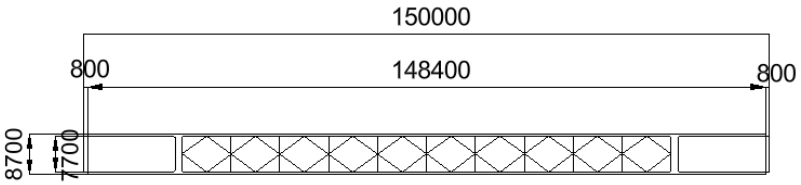

b) Plan view

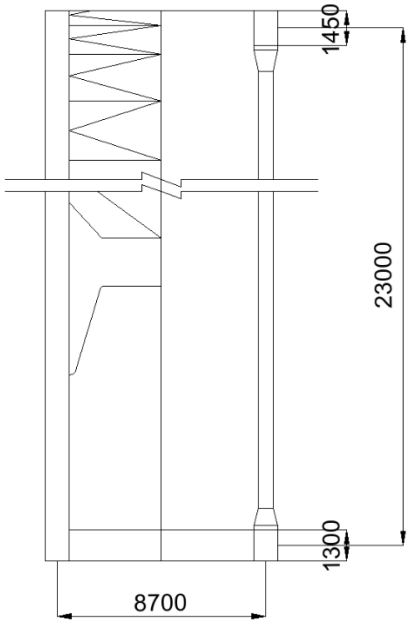

c) Sectional view

Fig.2 General arrangement drawing

The locations and photographs of the cracks are shown in Fig. 3. In general, cracks tend to occur in welded joints. However, the cracks found in this bridge were not located at the welds but rather near the gusset plates at the ends of the hangers. Since section loss due to corrosion was also observed in these areas, it was considered that the cracks were caused by the combined effect of bending and axial stresses induced by wind-induced vibration, along with stress concentration due to corrosion.

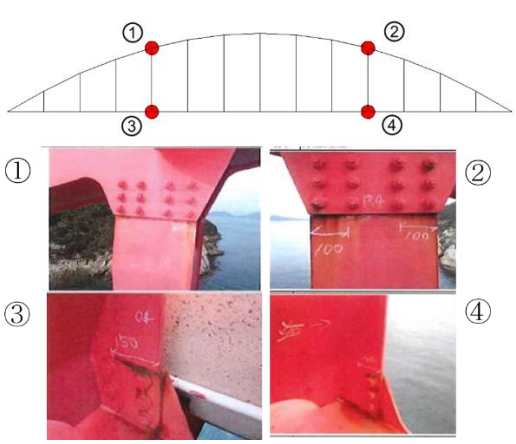

Fig.3 Found cracks

3. ANALYSIS

In this study, the vibration modes of the bridge were identified, and forced displacement analyses were performed by setting the maximum displacement in each mode to 20 mm, corresponding to the maximum displacement observed during a typhoon. Displacements proportional to the mode shape were applied to all the other nodes, and the bending stress at the crack location was calculated. Based on the results, the influence of each vibration mode on crack initiation was evaluated.

The commercial software MIDAS Civil was used for analysis. The bridge was modeled using three-dimensional elastic beam elements, as shown in Fig.4. The model consists of 286 nodes and 476 elements. The segments between nodes in this model were not subdivided, and each segment was represented by a single element. The green mark represents a support. The support conditions are described in the following paragraph. The validity of the model was verified by comparing its natural frequencies with those obtained from measured acceleration data.

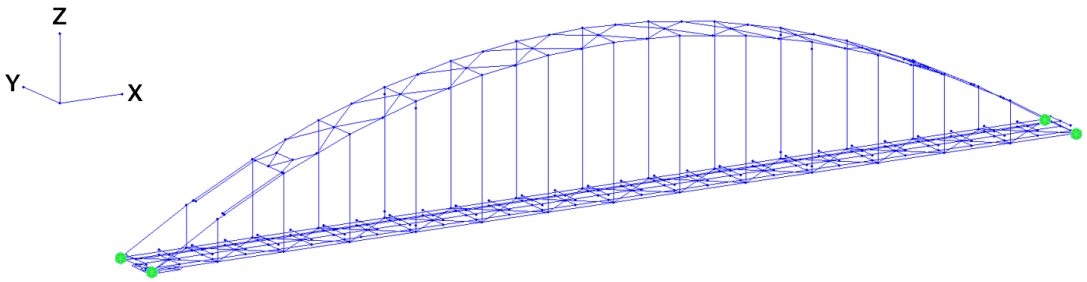

Fig.4 Global model

Two support conditions were considered for the entire bridge: one representing a healthy state, in which one end was modeled as a pinned support (restrained in all translational and rotational degrees of freedom, except for rotation about the Y-axis) and the other as a roller support (restrained in all directions except for translation in the X-direction and rotation about the Y-axis), and the other representing a deteriorated state, in which both ends were fully fixed (restrained in both translation and rotation).

The material properties of the components are listed in Table 1. In this model, the gusset plates and bolts were not explicitly modeled; therefore, the unit weight of steel was increased by 20% compared with the standard value for general steel materials to consider their mass.

To determine the natural frequencies of the entire bridge under two different boundary conditions, eigenvalue analyses were conducted.

Table 1 Material properties

	steel members	deck slab
modulus of elasticity (kN/m^2)	2.00×10^8	4.00×10^7
Poisson's ratio	0.3	0.2
unit weight (kN/m^3)	92.49	23.5

Eq. (1) was used to calculate the natural frequency of the cracked hanger.

$$f_n = \frac{1}{2\pi}\frac{\lambda_n^2}{L^2}\sqrt{\frac{EI}{\rho A}} \tag{1}$$

where λ_n is the constant for each eigenmode under fixed-fixed boundary conditions, L is the member length, E is the modulus of elasticity, I is the second moment of area, ρ is the unit weight, and A is the cross-sectional area of the member.

The natural frequencies of the entire bridge were calculated using eigenvalue analysis. These were then compared with the power spectrum of the strain obtained from the ambient vibration measurements to identify the likely vibrating modes. For each identified mode, a displacement shape similar to the mode shape was applied, such that the maximum vertical displacement matched the maximum displacement of 20 mm recorded by accelerometers during a typhoon. Using this displacement, the bending moment at the end of the cracked hanger was calculated.

The same analysis was performed using the reduced cross-section (corroded) model to determine the bending moment at the end of the cracked hanger. The amount of thickness loss was assumed to be 0.6 mm, which is the average thickness reduction observed in the corroded flange.

4. RESULTS

Table 2 lists the first-mode natural frequencies obtained from the eigenvalue analyses under two different support conditions along with the natural frequencies obtained from the ambient vibration measurements.

Table 2 First natural frequency of the entire bridge

Measured		0.56Hz
Analysis	Pinned and roller supports	0.40Hz
	Fixed-fixed support	0.57Hz

Based on these results, it is inferred that the actual support condition of the bridge has shifted from the ideal pinned-roller state to a behavior that is more similar to a fixed-fixed condition due to support deterioration. Therefore, in the subsequent forced-displacement analysis, both ends were fixed.

Prior to conducting the forced-displacement analysis, the higher-order vibration modes of the entire bridge were obtained, and the results are listed in Table 3. The power spectrum of the measured strain data is shown in Fig. 5. The strain gauge was positioned at the seaward flange edge on the lower end of the 4th hanger from the bearing where the crack was observed.

Table 3 Higher-order natural frequencies of the entire bridge

f_1	f_2	f_3	f_4	f_5	f_6	f_7
0.57Hz	0.97Hz	0.98Hz	1.19Hz	1.34Hz	1.71Hz	1.77Hz

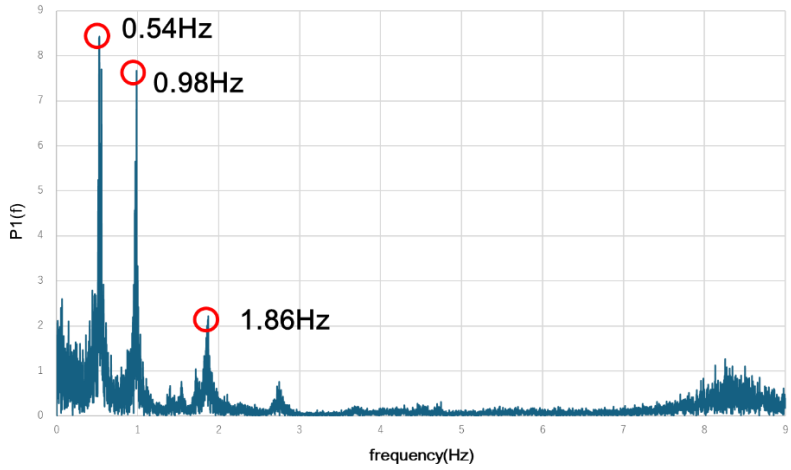

Fig.5 Strain power spectrum

Based on these results, it was determined that the bridge primarily vibrated in the 1st, 3rd, and 7th modes, which were used for the forced-displacement analyses.

The mode shapes are shown in Fig. 6.

The node with the maximum displacement in the entire bridge was identified for each mode based on the mode shape. A vertical displacement of 20 mm, corresponding to the maximum displacement observed during the typhoon, was applied to the node with the maximum displacement, that is at the 1/4 point for the 1st mode, 1/2 point for the 3rd mode, and 1/8 point for the 7th mode. Similar displacements proportional to each vibration mode were applied to all other nodes. Using the results of this analysis, the bending and axial stresses at the end of the cracked hanger were calculated under normal conditions from the bending moment and axial force, as listed in Table 4. The corresponding stresses under section-loss conditions are listed in Table 5.

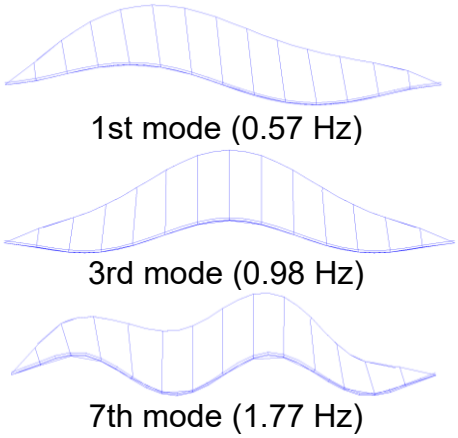

Fig. 6 Vibration mode diagram

Table 4 Stress range in the cracked hanger under intact condition

	Bending stress (N/mm^2)	Axial stress (N/mm^2)	Normal stress (N/mm^2)
First mode	30.4	-0.4	30.0
Third mode	-60.2	0.0	-60.2
Seventh mode	124.0	1.2	125.2

Table 5 Stress range in the cracked hanger under thinning condition

	Bending stress (N/mm^2)	Axial stress (N/mm^2)	Normal stress (N/mm^2)
First mode	32.0	-0.4	31.6
Third mode	-63.4	0.0	-63.4
Seventh mode	130.4	1.2	131.6

5. DISCUSSION ON THE CAUSES OF CRACK INITIATION

As shown in Tables 4 and 5, the axial stress at the crack initiation point is extremely low compared with the bending stress, suggesting that its contribution to crack initiation is negligible. Furthermore, the increase in the normal stress before and after wall thinning was approximately 5% across all the vibration modes. According to JRA (2004), the cut-off limit for variable stress ranges of grade C at the gas-cut edges of flange plates and structural steel is 53 N/mm^2.

Since the normal stress ranges in the 1st mode were below 53 N/mm^2, the vibration in this mode cannot be directly identified as the cause of the crack initiation. However, the normal stress ranges at the cracked hanger end in the 3rd and 7th modes exceeded 53 N/mm^2. In the 3rd mode, the normal stress range was 63.4 N/mm^2, approximately

20 % higher than 53 N/mm², suggesting that if vibrations occurred in this mode, they could have contributed to the crack initiation, whereas the 7th mode cannot be definitively considered the primary cause either since the power of this mode was approximately 1/4 of that of the 1st and 3rd modes, as shown in Fig. 5.

The natural frequencies of the cracked hanger from the 1st to the 5th mode, calculated using Eq. (1), are summarized in Table 6.

Table 6 Natural frequencies of the cracked hanger

f_1	f_2	f_3	f_4	f_5
10.23Hz	28.19Hz	55.25Hz	91.46Hz	136.59Hz

Since there was a possibility that axial stress might be amplified due to resonance, a comparison was made between the natural frequencies of the hanger and those of the entire bridge. As shown in Fig.5 and Table 6, the natural frequencies of the entire bridge and hanger did not exhibit closely matching values. Therefore, it is concluded that resonance does not occur between the vibrations of the entire bridge and those of the hanger.

6. CONCLUTIONS

In this study, forced displacement analyses were conducted by applying a displacement of 20 mm to the node with the maximum displacement in the vibration mode, whereas displacements proportional to the mode shape were applied to the other nodes. Through the analyses, the normal stress at the crack location, natural frequency of the entire bridge, and natural frequency of the cracked hanger were evaluated to estimate the cause of the crack initiation.

The main findings of this study are summarized as follows.

1) The eigenvalue analysis of the entire bridge revealed that the actual behavior of the bearings is not that of a pin-roller support, but rather resembles a fixed support at both ends.
2) The stresses observed in the cracked hanger members were primarily bending stresses, with those by axial force being negligible. At the current level of section loss due to corrosion, the increase in the normal stress was approximately 5%.
3) The normal stresses obtained from the analysis for the 1st vibration mode were small, indicating that the cracks were unlikely to be caused solely by the stresses induced by the overall vibration of the bridge.
4) The analysis revealed that the normal stress in the third mode was significant, suggesting that the stress induced by the overall vibration of the bridge may have contributed to the crack initiation.
5) Although the normal stresses obtained from the analysis for the 7th vibration mode were relatively large, it was determined that cracks could not be

attributed solely to the stress at that time, as displacement does not constantly occur.

6) It was confirmed that resonance did not occur as the natural frequency of the entire bridge and that of the cracked hanger member were sufficiently different.

REFERENCES

Japan Road Association (JRA) (2004), Specifications for Highway Bridges, (Part I: Common, Part II: Steel Bridges), Maruzen Publishing Co., Tokyo.

Miki, C.. Tateishi, K., Sakano, M., and Fukuoka, Y. (1988), “Data base for fatigue crackings in steel bridges”, Proceedings of the Japan Society of Civil Engineers., No.392/I-9.,403-410